AGU PUBLICATIONS

Geophysical Research Letters

RESEARCH LETTER
10.1002/2016GL071822

Key Points:
- Splash entrainment of sand and snow in saltation can be predicted using energy and momentum conservation laws
- The ejection regime of uniform sand is inherently different from that of heterogenous sand
- Cohesive snow shows a mixed ejection regime, statistically controlled either by energy or momentum balance depending on the impact velocity

Supporting Information:
- Supporting Information S1

Correspondence to:
F. Comola,
francesco.comola@gmail.com

Citation:
Comola, F., and M. Lehning (2017), Energy- and momentum-conserving model of splash entrainment in sand and snow saltation, *Geophys. Res. Lett.*, *44*, 1601–1609, doi:10.1002/2016GL071822.

Received 3 NOV 2016
Accepted 26 JAN 2017
Accepted article online 30 JAN 2017
Published online 13 FEB 2017

Energy- and momentum-conserving model of splash entrainment in sand and snow saltation

Francesco Comola[1] **and Michael Lehning**[1,2]

[1]School of Architecture, Civil and Environmental Engineering, Swiss Federal Institute of Technology, Lausanne, Switzerland, [2]WSL Institute for Snow and Avalanche Research SLF, Davos, Switzerland

Abstract Despite being the main sediment entrainment mechanism in aeolian transport, granular splash is still poorly understood. We provide a deeper insight into the dynamics of sand and snow ejection with a stochastic model derived from the energy and momentum conservation laws. Our analysis highlights that the ejection regime of uniform sand is inherently different from that of heterogeneous sand. Moreover, we show that cohesive snow presents a mixed ejection regime, statistically controlled either by energy or momentum conservation depending on the impact velocity. The proposed formulation can provide a solid base for granular splash simulations in saltation models, leading to more reliable assessments of aeolian transport on Earth and Mars.

1. Introduction

Saltation of sand-sized granular materials plays a key role in a wide range of environmental processes. Wind-driven sediment transport is responsible for dune and ripple development and erosion of geological features on Earth, Mars, Venus, and Titan [*Iversen and White*, 1982; *Kok et al.*, 2012]. In alpine terrain, drifting and blowing snow exert strong control on the snow depth distribution [*Mott et al.*, 2010], with relevant implications for hydrology and avalanching [*Lehning and Fierz*, 2008]. Furthermore, aeolian processes affect the surface mass balance in Antarctica, transporting a significant amount of snow from the ice sheets to the ocean [*Scarchilli et al.*, 2010].

The behavior of granular materials set to motion by aerodynamic forces was the subject of the early work of *Bagnold* [1941], which laid the basis for Owen's steady state saltation model [*Owen*, 1964]. Since then, the study of aeolian transport led to numerical models that embraced the full saltation process [*Anderson and Haff*, 1988, 1991; *McEwan and Willetts*, 1991, 1993; *Doorschot and Lehning*, 2002], generated experimental data sets against which these models were tested [*Willetts and Rice*, 1986; *Shao and Raupach*, 1992; *Rice et al.*, 1995, 1996; *Guala et al.*, 2008], and inspired theoretical advances that yet furthered the field [*Kok and Renno*, 2008; *Diplas et al.*, 2008; *Ho et al.*, 2011; *Carneiro et al.*, 2011, 2013].

It has been long known that the granular splash problem lies at the heart of aeolian saltation physics. After being accelerated by the wind, saltating grains impact the bed at high speed and low angle. The bed at the site of impact consists of grains that may differ in diameter and that may be glued to one another to differing degrees, by sintering in the case of snow or by menisci of water in the case of sand. The impact energy and momentum are partially retained by the impactor, which typically rebounds from the bed at lower speed and higher angle. The remaining energy and momentum are consumed in the ejection of other grains, typically 1–10, and in the frictional rearrangement of several other grains near the impact site. Recent studies indicated that splash entrainment is more efficient than aerodynamic forces in lifting grains from the surface, both for sand [*Walter et al.*, 2014] and snow [*Paterna et al.*, 2016]. The control exerted by splash entrainment is even stronger on Mars, where the lower gravity and air density allow grains to follow higher and longer ballistic trajectories, yielding larger impact velocities and thus more ejections per impact [*Parteli and Herrmann*, 2007; *Almeida et al.*, 2008; *Kok*, 2010]. This granular splash problem is highly stochastic, as it depends upon the size and velocity of the impacting grain, the size distribution in the granular bed, and the cohesion among grains near the impact site. One of the main challenges in the development of comprehensive aeolian saltation models is to arrive at a statistical representation of the splash process that accounts for all these relevant factors.

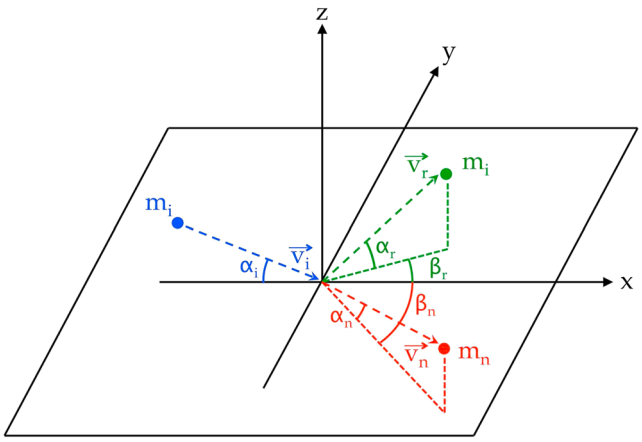

Figure 1. Schematic representation of the impact-ejection dynamics. The impacting particle (blue dot) has mass m_i and velocity v_i. Upon impact, the particle can rebound (green dot) with velocity v_r and eject other particles (red dot) of mass m_n and velocity v_n. The reference system is such that the vertical plane (x, z) contains the impact velocity vector $\vec{v}_i$, which forms an angle α_i with the horizontal plane (x, y). The rebound velocity vector $\vec{v}_r$ forms an angle α_r with the horizontal plane (x, y), and an angle β_r with the vertical plane (x, z). Similarly, the ejection velocity vector $\vec{v}_n$ forms an angle α_n with the horizontal plane (x, y), and an angle β_n with the vertical plane (x, z).

Here we attempt such a representation starting from fundamental conservation laws. The proposed formulation allows us to predict the number of ejections upon impact of a grain with given size and velocity. The model accounts for size distribution and cohesion of surface grains, such that it can be adapted to study the ejection regime of a wide range of granular materials. We employ the model to address long-standing problems related to aeolian transport. In particular, while the momentum balance proves statistically more restrictive than the energy balance in terms of the number of ejections from a loose granular bed [*Kok and Renno*, 2009], the opposite may be true for cohesive particles. Moreover, previous studies by *Anderson and Bunas* [1993] suggest that the multigrain size problem in splash entrainment lies at the heart of the reverse grading and migration of aeolian ripples. The ejection regimes of heterogeneous sand may in fact be inherently different from that of uniform sand due to the negative correlation between size and velocity of splashed grains. The proposed formulation can provide a solid base for simulations of splash entrainment in saltation models, ultimately leading to improved assessments of aeolian transport processes on Earth and Mars.

2. Ejection Model

Let us consider the impact of a single particle of mass m_i and velocity v_i with the granular bed. Upon impact, this particle has a probability $P_r \in [0; 1]$ of rebounding with velocity v_r. Moreover, a certain number of particles may be ejected from the granular bed. We define the reference system (x, y, z) such that the vertical plane (x, z) contains the impact velocity vector $\vec{v}_i$ (see Figure 1). Mass, velocity, and number of ejected particles are constrained by the energy and momentum conservation laws [*Kok and Renno*, 2009]. The energy balance equation reads

$$\sum_{n=1}^{N} \left(\frac{1}{2} m_n v_n^2 + \phi_n \right) = \left(1 - P_r \epsilon_r - \epsilon_f \right) \frac{1}{2} m_i v_i^2, \tag{1}$$

where N indicates the number of ejections; m_n and v_n are mass and velocity of the n^{th} ejected particle; ϕ_n is the cohesive bond exerted on the n^{th} particle by its neighboring particles; and ϵ_r is the fraction of impact energy retained by the rebounding particle, while ϵ_f is the fraction of impact energy lost to the bed.

Because the impact angle α_i is generally small, approximately 10° [*Bagnold*, 1941], most of the impact momentum is directed along x. The momentum balance equation in this direction reads

$$\sum_{n=1}^{N} \left(m_n v_n \cos\alpha_n \cos\beta_n \right) = \left(1 - P_r \mu_r - \mu_f \right) m_i v_i \cos\alpha_i, \tag{2}$$

where α_n and β_n are the vertical and horizontal ejection angles of each splashed particle; and μ_r is the fraction of impact momentum retained by the rebounding particle in the x direction, while μ_f is the fraction of impact momentum lost to the bed. Cohesive forces do not appear in equation (2), as the sum of pairwise

equal particle interactions acting in opposite directions always conserves momentum. By dividing both sides of equations (1) and (2) by N, we obtain

$$N = \frac{\left(1 - P_r\epsilon_r - \epsilon_f\right) m_i v_i^2}{\frac{1}{N}\sum_{n=1}^{N} m_n v_n^2 + 2\phi}, \tag{3}$$

$$N = \frac{\left(1 - P_r\mu_r - \mu_f\right) m_i v_i \cos\alpha_i}{\frac{1}{N}\sum_{n=1}^{N} m_n v_n \cos\alpha_n \cos\beta_n}, \tag{4}$$

where we have assumed a mean value of cohesion ϕ for all ejecta. The ejection problem is highly underdetermined, presenting just two equations and $2N+1$ unknowns, namely, N values of mass, N values of velocity, and the number of ejections N. Nevertheless, we may seek a solution by approximating the arithmetic means in equations (3) and (4) with the corresponding ensemble means $\langle mv^2\rangle$ and $\langle mv\cos\alpha\cos\beta\rangle$, which are equivalent to the arithmetic means in the limit $N \to \infty$. This approximation, in fact, allows us to exploit our knowledge of the probability distributions of ejecta's mass and velocity to solve the ejection problem. We therefore write

$$N_E = \frac{\left(1 - P_r\epsilon_r - \epsilon_f\right) m_i v_i^2}{\langle mv^2\rangle + 2\phi}, \tag{5}$$

$$N_M = \frac{\left(1 - P_r\mu_r - \mu_f\right) m_i v_i \cos\alpha_i}{\langle mv\cos\alpha\cos\beta\rangle}. \tag{6}$$

N_E and N_M are the number of ejections predicted by the energy and momentum balance, respectively. Because the approximated energy and momentum balances (equations (5) and (6)) generally yield two different solutions, i.e., $N_E \neq N_M$, a physically sensible ejection function must satisfy $N = \min\left(N_E, N_M\right)$, so that neither energy nor momentum are created [*Kok and Renno*, 2009; *McElwaine et al.*, 2004].

We further manipulate the mean values in equations (5) and (6) to account for the negative correlation between ejecta's size and velocity; that is,

$$\langle mv^2\rangle = \langle m\rangle\langle v^2\rangle + r_E\sigma_m\sigma_{v^2}, \tag{7}$$

$$\langle mv\cos\alpha\cos\beta\rangle = \langle m\rangle\langle v\rangle\langle\cos\alpha\rangle\langle\cos\beta\rangle + r_M\sigma_m\sigma_v, \tag{8}$$

where σ_m, σ_v, and σ_{v^2} are the standard deviations of m, v, and v^2, respectively; r_E is the correlation coefficient between m and v^2, and r_M is the correlation coefficient between m and v. The physical interpretation of these correlations is that heavier particles are likely to be ejected with smaller velocities due to their larger inertia. The effect of such negative correlations is to reduce the mean values in equations (5) and (6) and thus increase the total number of ejections necessary to close the energy and momentum balances.

Further manipulation can be carried out by considering well-established probability distributions for m and v. For granular beds, the particle sizes normally follow a lognormal distribution [*Kolmogorov*, 1941; *Colbeck*, 1986; *Barndorff-Nielsen*, 1986]. Moreover, the ejection velocity is usually well described by an exponential distribution [*Anderson and Haff*, 1988, 1991; *Mitha et al.*, 1986; *Beladjine et al.*, 2007]. Denoting with $\langle d\rangle$ and σ_d the mean and standard deviation of the ejecta's diameter, we obtain

$$N_E = \frac{\left(1 - P_r\epsilon_r - \epsilon_f\right) d_i^3 v_i^2}{2\langle v\rangle^2\left(\langle d\rangle + \frac{\sigma_d^2}{\langle d\rangle}\right)^3\left(1 + r_E\sqrt{5\left[1 + \left(\frac{\sigma_d}{\langle d\rangle}\right)^2\right]^9 - 5}\right) + 2\phi}, \tag{9}$$

$$N_M = \frac{\left(1 - P_r\mu_r - \mu_f\right) d_i^3 v_i \cos\alpha_i}{\langle v\rangle\left(\langle d\rangle + \frac{\sigma_d^2}{\langle d\rangle}\right)^3\left(\langle\cos\alpha\rangle\langle\cos\beta\rangle + r_M\sqrt{\left[1 + \left(\frac{\sigma_d}{\langle d\rangle}\right)^2\right]^9 - 1}\right)}, \tag{10}$$

where d_i is the impacting grain's diameter (we provide additional details on the derivation of equations (9) and (10) in section 1 in the supporting information). Equations (9) and (10) allow us to estimate the number of ejections upon impact of a grain of size d_i at velocity v_i. The novelty of the proposed approach stems from the possibility of accounting for the full spectrum of particle sizes, cohesion, and the negative correlation between ejection size and velocity, which has been observed experimentally and is likely to occur in natural saltation.

Table 1. Model Parameters

Parameter	Range in Literature	Value Used in the Model	Relevant Literature
ϵ_r	0.25–0.36	0.30	*Rice et al.* [1995], *Araoka and Maeno* [1981], *Nalpanis et al.* [1993], and *Nishimura and Hunt* [2000]
ϵ_f	0.61 – 0.72	0.67	*Ammi et al.* [2009]
μ_r	0.44–0.54	0.50	*Rice et al.* [1995] and *Nishimura and Hunt* [2000]
μ_f	0.37–0.44	0.40	*Rice et al.* [1995]
r_E[a]	Unclear	−0.30	*Rice et al.* [1995]
r_M[a]	Unclear	−0.40	*Rice et al.* [1995]
ϕ[b]	10^{-10}–10^{-8}	10^{-10}, 10^{-9}, 10^{-8}	*Gauer* [2001] and *Groot Zwaaftink et al.* [2014]
$\langle\cos\alpha\rangle$	0.76–0.83	0.80	*Willetts and Rice* [1986, 1989], *Rice et al.* [1995, 1996], *Nalpanis et al.* [1993], and *Nishimura and Hunt* [2000]
$\langle\cos\beta\rangle$	0.41–0.97	0.97	*Ammi et al.* [2009] and *Xing and He* [2013]
P_r	NA	Function of v_i (equation (S11))	*Anderson and Haff* [1991] and *Andreotti* [2004]
$\langle v\rangle$	NA	Function of v_i (equation (S12))	*Kok and Renno* [2009] and *Kok et al.* [2012]

[a]Estimates of the correlation coefficients are only available for sand (values $r_E = r_M = 0$ are assumed for snow).
[b]Estimates of cohesion apply only to snow (a value $\phi = 0$ J is used for loose sand). Equations (S11) and (S12) are given in the supporting information. NA means not applicable.

We can thus employ equations (9) and (10) to simulate the ejection process of a wide range of granular materials, both loose and cohesive. In particular, we apply our model to investigate the ejection regime of sand and snow, relying on the extensive literature data to assign well-established values to the model parameters.

The model formulation depends on a series of parameters, which we assign based on literature data. We summarize in Table 1 the model parameters, their range of variation estimated from published literature, and the value assumed in our simulations. In section 2 of the supporting information we provide additional details on the model parameters and the mathematical formulations of P_r and $\langle v\rangle$, which are commonly expressed as functions of the impact velocity v_i [*Anderson and Haff*, 1988; *Kok et al.*, 2012]. Furthermore, in section 3 of the supporting information, we show that the model is robust to variations of ±20% in the model parameters.

3. Sand Ejection

We first investigate the ejection regime of uniform sand, assigning $d_i = \langle d\rangle = 1$ mm, $\sigma_d = 0$ mm, and $\phi = 0$ J to be consistent with the experimental conditions of previous studies [*Werner*, 1987; *Anderson and Haff*, 1988]. It is worth noting that $\sigma_d = 0$ in equations (9) and (10) implies that the correlation coefficients r_E and r_M do not play a role. We study the mean ejection regime with the Monte Carlo method, to account for the variability

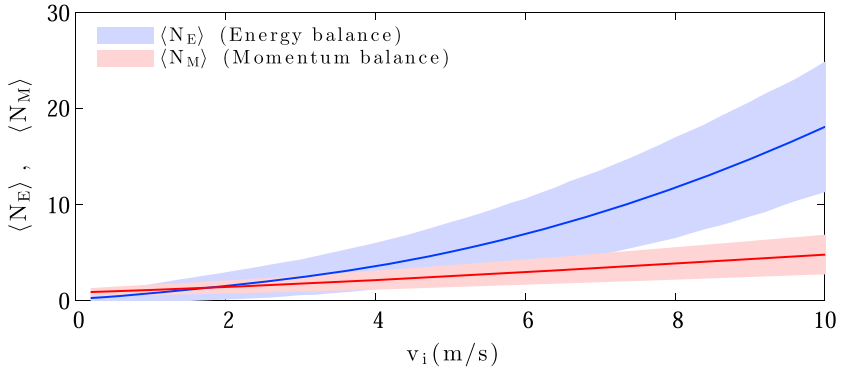

Figure 2. Mean number of ejections as predicted by equations (9) (blue line) and (10) (red line) for uniform sand with $\langle d\rangle = 1$ mm, $\sigma_d = 0$ mm, and $\phi = 0$ J. The shadowed bands represent the errors introduced with respect to the exact energy and momentum balance equations (3) and (4).

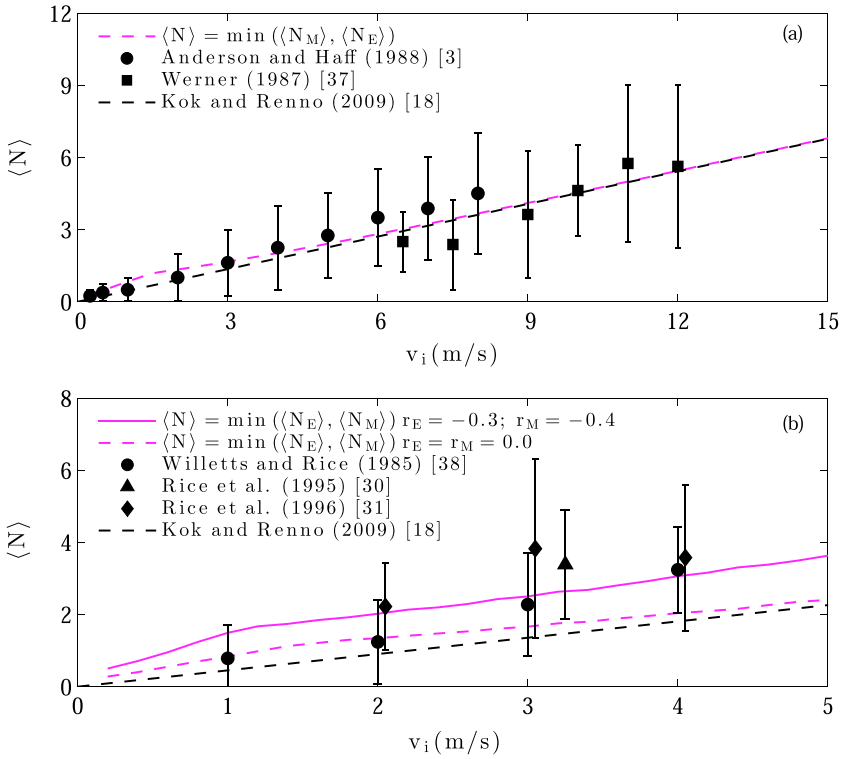

Figure 3. (a) Predicted number of ejections (magenta line) for uniform sand with $\langle d \rangle = 1$ mm and $\sigma_d = 0$ mm. Black squares refer to wind tunnel tests performed with uniform sand of size 800 μm [*Werner*, 1987]. Black circles refer to numerical simulations of uniform sand of size 1 mm [*Anderson and Haff*, 1988]. Vertical bars indicate standard deviations. The dashed black line is the ejection function of the COMSALT model [*Kok and Renno*, 2009]. (b) Predicted number of ejections for heterogeneous sand with $\langle d \rangle = 250$ μm, $\sigma_d = 50$ μm, including (solid magenta line) and neglecting (dashed magenta line) the negative correlation between ejecta's mass and velocity. The black markers refer to wind tunnel studies carried out with a mixture of fine (150–250 μm), medium (250–355 μm), and coarse (355–600 μm) sand fractions [*Willetts and Rice*, 1985; *Rice et al.*, 1996, 1995]. Vertical bars indicate standard deviations. Results of the COMSALT model (dashed black line) are shown as reference simulation of uniform sand ejection. Experiments [*Oger et al.*, 2005; *Beladjine et al.*, 2007; *Ammi et al.*, 2009; *Mitha et al.*, 1986] and models [*Crassous et al.*, 2007] from sediments other than sand are omitted because different sphericity, elasticity, and friction coefficients are likely to produce different ejection regimes.

in impact velocity and impact direction. Specifically, for increasing values of impact velocity v_i, we carry out stochastic sampling of the impact angle α_i, calculating the number of ejecta with equations (9) and (10) (see section 4 in the supporting information for additional details on the Monte Carlo procedure). We then average the values of N_E and N_M resulting from each simulation to provide the mean ejection numbers $\langle N_E \rangle$ and $\langle N_M \rangle$.

Figure 2 shows the trends of $\langle N_E \rangle$ and $\langle N_M \rangle$ in the range of impact velocity typical of natural saltation. The results indicate that the momentum balance is statistically more restrictive than the energy balance in terms of mean number of ejections. Momentum balance is therefore what is expected to control the number of ejections in uniform sand saltation, as was observed in a previous analysis [*Kok and Renno*, 2009]. Moreover, the momentum-conserving solution shows a linear increase of $\langle N \rangle$ with impact velocity, which is consistent with several previous studies [*Werner*, 1990; *McEwan and Willetts*, 1991]. The shaded areas in Figure 2 correspond to the mean error introduced by solving equations (5) and (6) in place of equations (3) and (4), which we solve by sequential sampling of ejected particles until we reach the balances of energy and momentum. In principle, the error introduced when replacing arithmetic means with ensemble means is larger for small values of N, i.e., when the impact velocity is small. Under the same circumstances, however, both the ensemble and the arithmetic means are close to zero due to the small ejection velocity, thus balancing the mean error across the whole range of N. Figure 3a shows the momentum- and energy-conserving solution $\langle N \rangle = \min\left(\langle N_E \rangle, \langle N_M \rangle\right)$ for uniform sand (magenta line), which proves consistent with previous experimental and numerical data [*Werner*, 1987; *Anderson and Haff*, 1988] (black markers) as well as with state-of-the-art parameterizations for sand ejections (black line) [*Kok and Renno*, 2009].

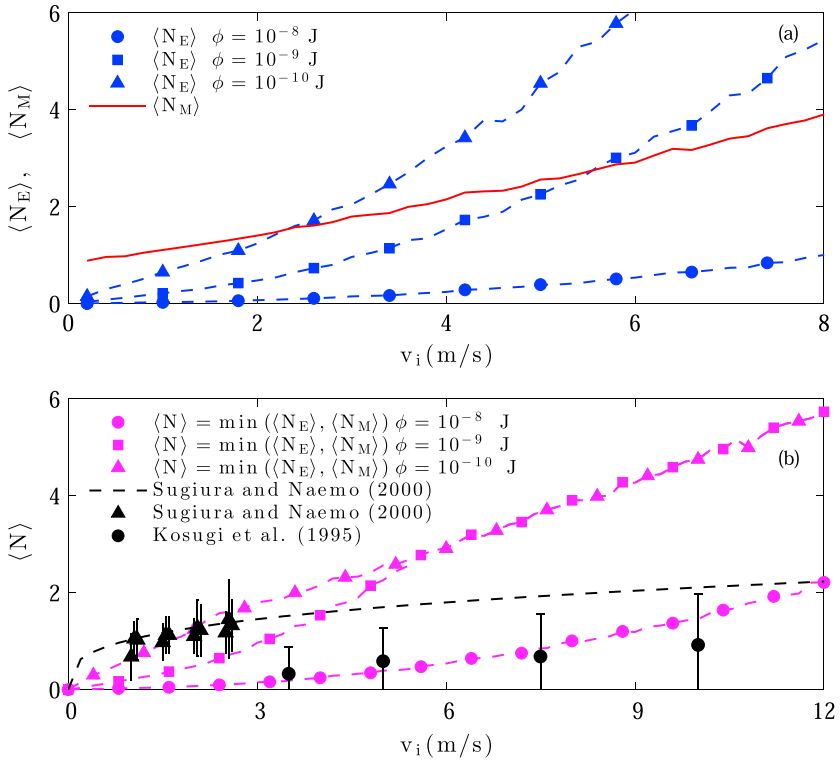

Figure 4. (a) Number of snow ejections predicted by the momentum balance equation (10) (red line) and by the energy balance equation (9), for different values of cohesion ϕ (blue lines). Snow size distribution parameters are $\langle d \rangle = 200\,\mu m$ and $\sigma_d = 100\,\mu m$. (b) Predicted number of snow ejections (magenta lines) resulting from the lower envelopes of the red and blue lines in Figure 4a. Black triangles refer to wind tunnel studies on ejection of both fresh and compact snow [*Sugiura and Maeno*, 2000]. Black circles refer to ejection experiments carried out with densely packed ice particles and for impact angles between 5° and 15°, typical of saltation [*Kosugi et al.*, 1995]. Vertical bars indicate standard deviations. The dashed black line refers to the empirical ejection function obtained by fitting a power law to the compact snow data [*Sugiura and Maeno*, 2000].

We further apply the model to simulate the ejection regime of heterogeneous sand. To our knowledge, among all experimental investigations carried out with heterogeneous sand, only *Rice et al.* [1995] successfully measured the ejection velocity of grains of different size, highlighting the existence of negative correlations. Accounting for all the experimental tests reported in *Rice et al.* [1995], we estimate overall correlation coefficients $r_E \approx -0.3$ and $r_M \approx -0.4$. To reproduce the experimental conditions, we assign $\langle d \rangle = 250\,\mu m$ and $\sigma_d = 50\,\mu m$. The granular splash resulting from a heterogeneous bed differs greatly depending upon the size of the impactor. To handle both the role of the sorting at the site of the impact and the size of the impactor, we carry out a series of Monte Carlo simulations similar to those performed for uniform sand, but with the additional random sampling of the impact diameter. In particular, we sample d_i from the lognormal distribution of ejected grains, truncated within 70 and 500 μm, accounting for the fact that smaller grains are mostly in suspension and larger ones in reptation [*Shao*, 2008]. Figure 3b shows that the mean number of ejections obtained with $r_E = -0.3$ and $r_M = -0.4$ (solid magenta line) deviates significantly from that obtained with $r_E = r_M = 0.0$ (dashed magenta line), leading to a more accurate prediction of the experimental data for heterogeneous sand. Existing ejection models [*Kok and Renno*, 2009] (dashed black line) that do not account for such negative correlations fail to capture the larger ejection numbers measured for heterogeneous sand.

4. Snow Ejection

We consider typical snow properties by assigning $\langle d \rangle = 200\,\mu m$ and $\sigma_d = 100\,\mu m$. Because the correlation between mass and velocity of ejected snow has never been experimentally quantified, we focus the analysis only on the effect of cohesion and assign $r_E = r_M = 0$ for simplicity. Previous energy-conserving models of snow ejection [*Gauer*, 2001; *Groot Zwaaftink et al.*, 2014] suggest that ϕ may span the range 10^{-10}–10^{-8} J, depending on sintering among ice grains. We carry out Monte Carlo simulations following the same

random sampling procedure adopted for the heterogeneous sand case. Figure 4a shows the variation of $\langle N_E \rangle$ for three different values of cohesion. For $\phi = 10^{-10}$ J, there is a threshold value of impact velocity dividing a lower range in which the ejection regime is limited by the energy balance from an upper range in which the momentum balance is the main control. For $\phi = 10^{-9}$ J the threshold impact velocity increases significantly and for strongly sintered snow, with $\phi = 10^{-8}$ J, the energy balance limits the number of ejections across the whole range of impact velocity. These results confirm and extend previous observations [*Dietrich*, 1977] suggesting that the impact energy exerts a major control on ejection of cohesive materials. As suggested by equations (9) and (10), cohesion acts as a sink of impact energy but not of impact momentum, such that energy conservation becomes the principal constraint to granular splash of highly cohesive materials.

Figure 4b shows the predicted number of ejections $\langle N \rangle = \min\left(\langle N_E \rangle, \langle N_M \rangle\right)$ for the three tested values of ϕ together with experimental data on snow [*Sugiura and Maeno*, 2000] and ice particle ejection [*Kosugi et al.*, 1995]. The snow ejection measurements, carried out with both fresh and compact snow cover, lie close to the curve corresponding to $\phi = 10^{-10}$ J, while the data points obtained for densely packed ice particles lie close to the curve corresponding to $\phi = 10^{-8}$ J. The empirical ejection function obtained by fitting a power law to the compact snow data (dashed black line) [*Sugiura and Maeno*, 2000], commonly adopted in snow transport models, significantly deviates from the momentum-conserving solution for large values of impact velocities.

5. Conclusions

In aeolian saltation, wind-blown grains follow ballistic trajectories close to the surface and frequently impact the granular bed to generate what is called the granular splash. Surface grains may be loose, as in the case of dry sand, or bound to one another, by sintering in the case of snow or by water menisci in the case of wet sand. The impacting grain typically rebounds from the bed, retaining part of the impact energy and momentum. The remaining energy and momentum drive the frictional rearrangement of several grains near the impact site and the ejection of other grains, which is the most efficient entrainment mechanism in aeolian transport on Earth and Mars.

Our proposed ejection model provides a deeper insight into sediment transport. Our results confirm that momentum balance is the main control on loose sand ejection and that the number of ejecta per impact scales linearly with the impact velocity (Figure 2). We also show that the relatively larger ejection rate observed in experiments carried out with heterogeneous sand is successfully explained by our theory that includes a negative correlation between size and velocity of ejected grains (Figure 3). The correlation coefficients estimated from experimental results by *Rice et al.* [1995] yield a good match between modeled and measured number of ejections. This suggests that the ejection regime of heterogeneous sand is inherently different from that of uniform sand, for which the correlations do not play a role because $\sigma_d = 0$ (see equations (9) and (10)). In fact, when negative correlation coefficients are considered, the predicted number of ejection is almost twice as large as that obtained for uniform sand. Such a larger ejection efficiency is likely to influence the self-balanced transfer of momentum among fluid and saltating particles, leading to a larger separation between the wind speed required for aerodynamic entrainment and that required for continuation of transport.

Our model simulations of snow ejection highlight that cohesion produces a mixed ejection regime, statistically controlled by energy conservation below a threshold impact velocity and by momentum conservation above it (Figure 4). We observe that the threshold impact velocity increases with increasing cohesion. Our model suggests that the reason for such behavior lies in the effect of cohesion, as the breaking of bonds in the substrate dissipates impact energy but does not affect momentum conservation. However, the general, yet not well supported, opinion that energy conservation is the sole control on snow ejection may be a misconception, as there exists a large range of cohesion values for which momentum conservation controls ejection at high impact velocity.

Saltation models commonly track the trajectories of wind-blown particles, explicitly solving for their size d_i and velocity v_i upon impact with the granular bed [*Nemoto and Nishimura*, 2004; *Vinkovic et al.*, 2006; *Kok and Renno*, 2009; *Dupont et al.*, 2013; *Groot Zwaaftink et al.*, 2014]. Accordingly, these models may directly benefit from the proposed splash function, ultimately leading to improved simulations of larger-scale processes such as saltation intermittency and both ripple and dune development. Our results also point toward future needs in terms of experimental work for more precise quantifications of the model parameters, in particular, concerning the dependence of snow cohesive properties on temperature and relative humidity.

Acknowledgments
We thank Jasper F. Kok, Henning Löwe, Johan Gaume, and Christine Groot Zwaaftink for insightful discussions. We also wish to thank Robert S. Anderson and the anonymous reviewers for their constructive comments. All data used in this study will be made available upon request. The model results shown in Figures 2–4 are available at http://www.envidat.ch/dataset/resources/2016gl071822.

References

Almeida, M. P., E. J. Parteli, J. S. Andrade, and H. J. Herrmann (2008), Giant saltation on Mars, *Proc. Natl. Acad. Sci. U.S.A.*, *105*(17), 6222–6226.
Ammi, M., L. Oger, D. Beladjine, and A. Valance (2009), Three-dimensional analysis of the collision process of a bead on a granular packing, *Phys. Rev. E*, *79*(2), 021305.
Anderson, R. S., and K. L. Bunas (1993), Grain size segregation and stratigraphy in aeolian ripples modelled with a cellular automaton, *Nature*, *365*, 740–743.
Anderson, R. S., and P. K. Haff (1988), Simulation of eolian saltation, *Science*, *241*(4867), 820–823.
Anderson, R. S., and P. K. Haff (1991), Wind modification and bed response during saltation of sand in air, in *Aeolian Grain Transport 1*, edited by O. E. Barndorff-Nielsen and B. B. Willetts, pp. 21–51, Springer, Vienna.
Andreotti, B. (2004), A two-species model of aeolian sand transport, *J. Fluid Mech.*, *510*, 47–70.
Araoka, K., and N. Maeno (1981), Dynamical behaviors of snow particles in the saltation layer, *Mem. Natl. Inst. Polar Res. Spec. Issue Jpn.*, *19*, 253–263.
Bagnold, R. A. (1941), *The Physics of Blown Sand and Desert Dunes*, Methuen, London.
Barndorff-Nielsen, O. E. (1986), Sand, wind and statistics: Some recent investigations, *Acta Mech.*, *64*(1–2), 1–18.
Beladjine, D., M. Ammi, L. Oger, and A. Valance (2007), Collision process between an incident bead and a three-dimensional granular packing, *Phys. Rev. E*, *75*(6), 061305.
Carneiro, M. V., T. Pähtz, and H. J. Herrmann (2011), Jump at the onset of saltation, *Phys. Rev. Lett.*, *107*, 098001.
Carneiro, M. V., N. A. Araújo, T. Pähtz, and H. J. Herrmann (2013), Midair collisions enhance saltation, *Phys. Rev. Lett.*, *111*(5), 058001.
Colbeck, S. (1986), Statistics of coarsening in water-saturated snow, *Acta Metall. Mater.*, *34*(3), 347–352.
Crassous, J., D. Beladjine, and A. Valance (2007), Impact of a projectile on a granular medium described by a collision model, *Phys. Rev. Lett.*, *99*(24), 248001.
Dietrich, R. (1977), Impact abrasion of harder by softer materials, *J. Geol.*, *85*, 242–246.
Diplas, P., C. L. Dancey, A. O. Celik, M. Valyrakis, K. Greer, and T. Akar (2008), The role of impulse on the initiation of particle movement under turbulent flow conditions, *Science*, *322*(5902), 717–720.
Doorschot, J. J., and M. Lehning (2002), Equilibrium saltation: Mass fluxes, aerodynamic entrainment, and dependence on grain properties, *Boundary Layer Meteorol.*, *104*(1), 111–130.
Dupont, S., G. Bergametti, B. Marticorena, and S. Simoëns (2013), Modeling saltation intermittency, *J. Geophys. Res. Atmos.*, *118*, 7109–7128, doi:10.1002/jgrd.50528.
Gauer, P. (2001), Numerical modeling of blowing and drifting snow in alpine terrain, *J. Glaciol.*, *47*(156), 97–110.
Groot Zwaaftink, C. D., M. Diebold, S. Horender, J. Overney, G. Lieberherr, M. B. Parlange, and M. Lehning (2014), Modelling small-scale drifting snow with a lagrangian stochastic model based on large-eddy simulations, *Boundary Layer Meteorol.*, *153*(1), 117–139.
Guala, M., C. Manes, A. Clifton, and M. Lehning (2008), On the saltation of fresh snow in a wind tunnel: Profile characterization and single particle statistics, *J. Geophys. Res.*, *113*, F03024, doi:10.1029/2007JF000975.
Ho, T. D., A. Valance, P. Dupont, and A. Ould El Moctar (2011), Scaling laws in Aeolian sand transport, *Phys. Rev. Lett.*, *106*(9), 094501.
Iversen, J. D., and B. R. White (1982), Saltation threshold on Earth, Mars and Venus, *Sedimentology*, *29*(1), 111–119.
Kok, J. F. (2010), Difference in the wind speeds required for initiation versus continuation of sand transport on Mars: Implications for dunes and dust storms, *Phys. Rev. Lett.*, *104*(7), 074502.
Kok, J. F., and N. O. Renno (2008), Electrostatics in wind-blown sand, *Phys. Rev. Lett.*, *100*(1), 014501.
Kok, J. F., and N. O. Renno (2009), A comprehensive numerical model of steady state saltation (comsalt), *J. Geophys. Res.*, *114*, D17204, doi:10.1029/2009JD011702.
Kok, J. F., E. J. Parteli, T. I. Michaels, and D. B. Karam (2012), The physics of wind-blown sand and dust, *Rep. Prog. Phys.*, *75*(10), 106901.
Kolmogorov, A. (1941), On the logarithmic normal distribution of particle sizes under grinding, *Dokl. Akad. Nauk SSSR*, *31*, 99–101.
Kosugi, K., K. Nishimura, and N. Maeno (1995), Studies on the dynamics of saltation in drifting snow, *Rep. Natl. Res. Inst. Earth Sci. Disaster Prevention*, *54*, 111–154.
Lehning, M., and C. Fierz (2008), Assessment of snow transport in avalanche terrain, *Cold Reg. Sci. Technol.*, *51*(2), 240–252.
McElwaine, J. N., N. Maeno, and K. Sugiura (2004), The splash function for snow from wind-tunnel measurements, *Ann. Glaciol.*, *38*(1), 71–78.
McEwan, I., and B. Willetts (1991), Numerical model of the saltation cloud, in *Aeolian Grain Transport 1*, edited by O. E. Barndorff-Nielsen and B. B. Willetts, pp. 53–66, Springer, Vienna.
McEwan, I. K., and B. B. Willetts (1993), Adaptation of the near-surface wind to the development of sand transport, *J. Fluid Mech.*, *252*, 99–115.
Mitha, S., M. Tran, B. Werner, and P. K. Haff (1986), The grain-bed impact process in aeolian saltation, *Acta Mech.*, *63*(1–4), 267–278.
Mott, R., M. Schirmer, M. Bavay, T. Grünewald, and M. Lehning (2010), Understanding snow-transport processes shaping the mountain snow-cover, *Cryosphere*, *4*(4), 545–559.
Nalpanis, P., J. Hunt, and C. Barrett (1993), Saltating particles over flat beds, *J. Fluid Mech.*, *251*, 661–685.
Nemoto, M., and K. Nishimura (2004), Numerical simulation of snow saltation and suspension in a turbulent boundary layer, *J. Geophys. Res.*, *109*, D18206, doi:10.1029/2004JD004657.
Nishimura, K., and J. Hunt (2000), Saltation and incipient suspension above a flat particle bed below a turbulent boundary layer, *J. Fluid Mech.*, *417*, 77–102.
Oger, L., M. Ammi, A. Valance, and D. Beladjine (2005), Discrete element method studies of the collision of one rapid sphere on 2d and 3d packings, *Eur. Phys. J. E*, *17*(4), 467–476.
Owen, P. R. (1964), Saltation of uniform grains in air, *J. Fluid Mech.*, *20*(02), 225–242.
Parteli, E. J., and H. J. Herrmann (2007), Saltation transport on Mars, *Phys. Rev. Lett.*, *98*(19), 198001.
Paterna, E., P. Crivelli, and M. Lehning (2016), Decoupling of mass flux and turbulent wind fluctuations in drifting snow, *Geophys. Res. Lett.*, *43*, 4441–4447, doi:10.1002/2016GL068171.
Rice, M., B. Willetts, and I. McEwan (1995), An experimental study of multiple grain-size ejecta produced by collisions of saltating grains with a flat bed, *Sedimentology*, *42*(4), 695–706.
Rice, M., B. Willetts, and I. McEwan (1996), Observations of collisions of saltating grains with a granular bed from high-speed cine-film, *Sedimentology*, *43*(1), 21–31.
Scarchilli, C., M. Frezzotti, P. Grigioni, L. De Silvestri, L. Agnoletto, and S. Dolci (2010), Extraordinary blowing snow transport events in east Antarctica, *Clim. Dyn.*, *34*(7–8), 1195–1206.
Shao, Y. (2008), *Physics and Modelling of Wind Erosion, Atmos. and Oceanogr. Sci. Lib.*, Springer, Netherlands.
Shao, Y., and M. Raupach (1992), The overshoot and equilibration of saltation, *J. Geophy. Res.*, *97*(D18), 20,559–20,564.

Sugiura, K., and N. Maeno (2000), Wind-tunnel measurements of restitution coefficients and ejection number of snow particles in drifting snow: Determination of splash functions, *Boundary Layer Meteorol.*, *95*(1), 123–143.
Vinkovic, I., C. Aguirre, M. Ayrault, and S. Simoëns (2006), Large-eddy simulation of the dispersion of solid particles in a turbulent boundary layer, *Boundary Layer Meteorol.*, *121*(2), 283–311.
Walter, B., S. Horender, C. Voegeli, and M. Lehning (2014), Experimental assessment of Owen's second hypothesis on surface shear stress induced by a fluid during sediment saltation, *Geophys. Res. Lett.*, *41*, 6298–6305, doi:10.1002/2014GL061069.
Werner, B. (1990), A steady-state model of wind-blown sand transport, *J. Geol.*, *98*, 1–17.
Werner, B. T. (1987), A physical model of wind-blown sand transport, PhD thesis, California Inst. of Technol., Pasadena, Calif.
Willetts, B., and M. Rice (1985), Inter-saltation collisions, in *Proc. Int. Workshop on Physics of Blown Sand*, vol. 1, edited by O. E. Barndorff-Nielsen et al., pp. 83–100, Dep. Theor. Statist., Aarhus University, Aarhus, Denmark.
Willetts, B., and M. Rice (1986), Collisions in aeolian saltation, *Acta Mech.*, *63*(1–4), 255–265.
Willetts, B., and M. Rice (1989), Collisions of quartz grains with a sand bed: The influence of incident angle, *Earth Surf. Processes Landforms*, *14*(8), 719–730.
Xing, M., and C. He (2013), 3d ejection behavior of different sized particles in the grain-bed collision process, *Geomorphology*, *187*, 94–100.